Nanoporous Gold Film Prepared by the Epoxidation of Poly(styrene-*b*-butadiene) Diblock Copolymer Templated Micelles

Shiao-Wei Kuo,* Hong-Yi Yang, Chih-Feng Wang, Kwang-Un Jeong

A new approach is developed for the preparation of nanoporous gold (Au) films using diblock copolymer micelles as templates. Stable Au nanoparticles (NPs) with a narrow distribution are prepared by modifying NPs functionalized with 4-(dimethylamino)pyridine ligands (DMAP Au NPs) and a spherical micelle formed through the epoxidation of poly(styrene-*b*-butadiene) diblock copolymer to produce poly(styrene-*b*-vinyl oxirane) (PS-*b*-PBO) in tetrahydrofuran–acetonitrile solution. The exchange reaction of 4-aminothiophenol of PS-*b*-PBO diblock copolymer micelles with DMAP Au NPs can produce block copolymer–Au NPs composite films. After the pyrolysis of the diblock copolymer templates at a specific temperature to avoid the collapse of the Au NPs, a nanoporous Au film is prepared.

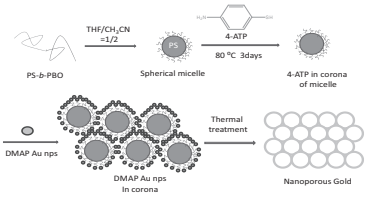

1. Introduction

In recent years, ordered nanoporous materials with a high surface area, large pore volume, and good mechanical stability have received much attention for their potential applications in adsorption, separation, catalysis, photonics, and drug delivery.[1–3] For example, high-surface-area nanoporous gold (Au) has attracted a great deal of interest for use as catalysts, sensors, and actuators.[4,5] Compared with a Au-nanoparticle (NP)-modified electrode, the nanoporous Au has a much higher surface area and better electron transport,[5] and it can be prepared by electrochemical deposition,[6] dealloying of Ag from Ag/Au alloys,[7] liquid crystal template technique,[8] and organic templating.[9,10] More recently, nanoporous Au could have the potential application in carbon monoxide oxidation, methanol elecrooxidation, and reduction of oxygen and hydrogen peroxide at ambient temperature.[11] By templating the self-assembly of small molecules, surfactant, and block copolymers, nanoporous structures with different sizes can be prepared.[12–14] The porous structure generated by template removal has pore sizes in the range of 10 nm to 1 μm. Wiesner and co-workers[15] reported that the self-assembly of a block copolymer and ligand-stabilized platinum NPs at a high NP loading produced an ordered mesoporous platinum–carbon nanocomposite with open and large pores (>10 nm) after the pyrolysis of the inverse hexagonal hybrid mesostrucuture.

In this study, we report on nanoporous Au films prepared using the epoxidation of poly(styrene-*b*-butadiene) (PS-*b*-PBO) diblock copolymer[16] templated micelles, as shown in Scheme 1. In the first step, we prepared 4-(dimethylamino)pyridine Au NPs (DMAP Au NPs) using a method by Gandubert and Lennox.[17] Next, an exchange reaction of 4-aminothiophenol (4-ATP) of the PS-*b*-PBO diblock copolymer micelles with DMAP Au NPs

S.-W. Kuo, H.-Y. Yang
Department of Materials and Optoelectronic Science, Center for Nanoscience and Nanotechnology, National Sun Yat-Sen University, Kaohsiung, Taiwan
E-mail: kuosw@faculty.nsysu.edu.tw
C.-F. Wang
Department of Materials Science and Engineering, I-Shou University, Kaohsiung, Taiwan
K.-U. Jeong
Department of Polymer-Nano Science and Technology, Chonbuk National University, Jeonju, Korea

DOI: 10.1002/macp.201100493

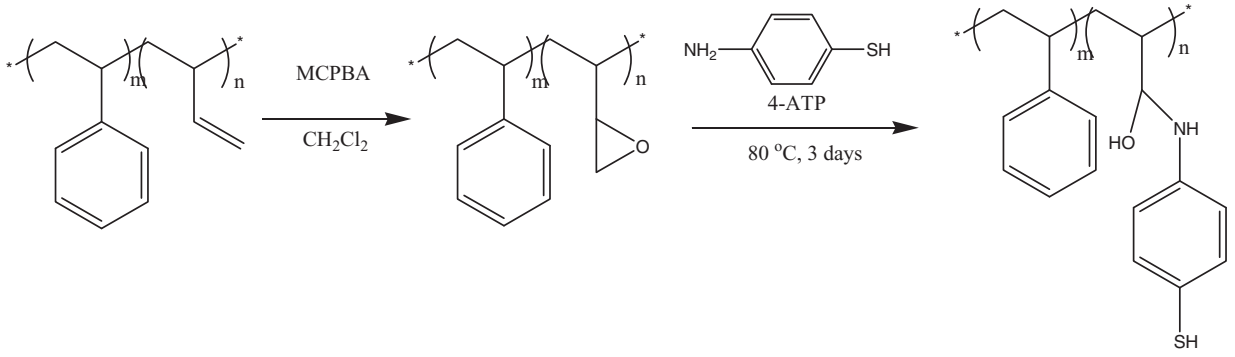

Scheme 1. The chemical structures of PS-*b*-PBO and 4-ATP with PS-*b*-PBO.

was performed to generate the block copolymer–Au NPs composite films. Finally, pyrolysis of the block copolymers at a specific temperature to avoid the collapse of the Au film produced a nanoporous Au film, as shown in Scheme 2.

2. Experimental Section

2.1. Materials

The diblock polymer used in this study, poly(styrene-*b*-butadiene (1,2 addition)) (PS-*b*-PB), with a polydispersity index of $\overline{M}_w/\overline{M}_n$ = 1.09 was synthesized by sequential anionic polymerization of styrene and butadiene (purchased from Polymer Source, Inc.). The degree of polymerization of styrene and butadiene was 1906 and 1796, respectively. 4-ATP, DMAP, *meta*-chloroperoxybenzoic acid, dichloromethane, chloroauric acid ($HAuCl_4$), tetraoctylammonium bromide (TOAB), sodium borohydride ($NaBH_4$), and toluene were purchased from Acros Organics.

2.2. Epoxidation of PS-*b*-PBO

PS-*b*-PB diblock copolymer was dissolved at an ambient temperature in dichloromethane (≈0.7 M) and then cooled to 0 °C. The solution was stirred for 10 min, and then 0.1 M *meta*-chloroperoxybenzoic acid was added to the PS-*b*-PB diblock solution. After stirring the solution for 72 h at 0 °C, the diblock polymer was recovered by precipitation in methanol and dried under high vacuum. The epoxidation of PS-*b*-PBO diblock copolymer generated poly(styrene-*b*-vinyl oxirane) (PS-*b*-PBO). The chemical scheme is provided in Scheme 1.

2.3. Preparation of the PS-*b*-PBO Micelle Solution and the Reaction Between PS-*b*-PBO and 4-ATP

The diblock copolymer (1 wt%) was first dissolved in tetrahydrofuran (THF), a common solvent for both PS and PBO blocks. The second solvent (acetonitrile, CH_3CN) was added slowly to the stirred polymer solution via a syringe, pumped at a constant rate.

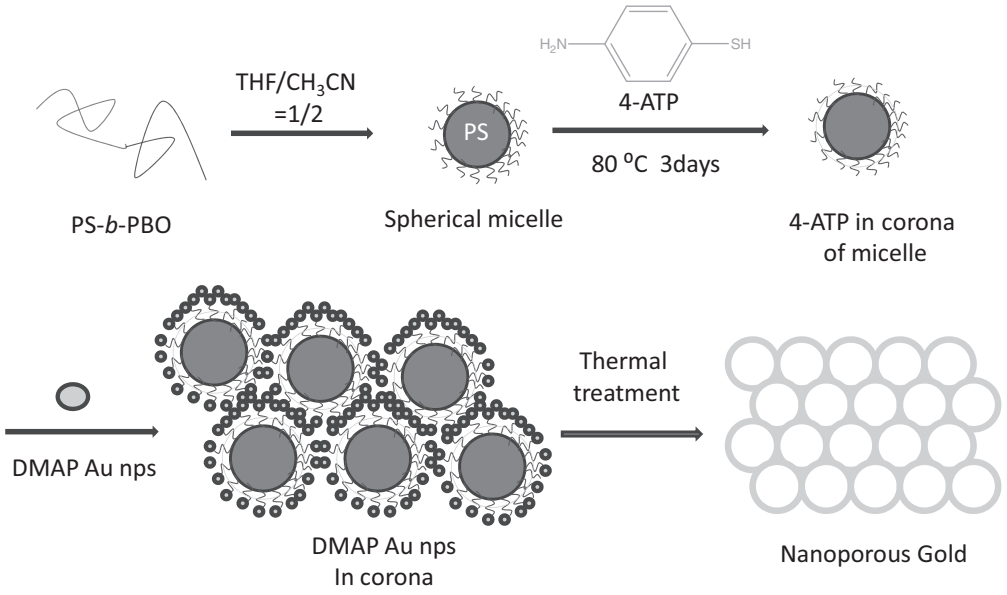

Scheme 2. The synthetic for the preparation of a nanoporous Au film.

A typical addition rate was 1–5 mL h^{-1}. To estimate the ideal solvent composition for the formation of micelles, the addition of solvent was continued until the solution became turbid during the first trial. In subsequent experiments, the addition was stopped before the appearance of turbidity (ca. THF–CH_3CN = 1:2). Stirring of solution was continued for 2 d prior to further characterization of PS-*b*-PBO micelles. The reaction between PS-*b*-PBO micelle and 4-ATP, as shown in Scheme 1, was performed in the following manner: stoichiometric amounts of 4-ATP with PS-*b*-PBO diblock copolymer micelle solution (molar ratio = 1:1) were mixed in a high-speed stirrer. The solution was allowed to react at 80 °C for 3 d.

2.4. Synthesis of DMAP Au NPs

The DMAP Au NPs used in this study were prepared using the method by Gandubert and Lennox.[17] A typical synthesis is as follows: 30 mL of an aqueous solution of $HAuCl_4$ (0.24 mmol) was stirred with a solution of TOAB (0.34 g) in 80 mL of toluene until all the $HAuCl_4$ had transferred to the organic layer. An aqueous solution of $NaBH_4$ was added slowly while stirring. Subsequently, an aqueous solution of DMAP was added to the solution of TOAB–Au NPs in toluene. Phase transfer of the particle occurred spontaneously, and the ruby red aqueous solution of DMAP-stabilized Au NPs was obtained.

2.5. Exchange Reaction Between PS-*b*-PBO–ATP with DMAP Au NPs and Preparation of Nanoporous Au Film

A toluene solution containing stoichiometric amounts (4:3, 4:4, 4:6, and 4:8) of PS-*b*-PBO–ATP micelle and DMAP Au NPs was mixed in a high-speed stirrer for few minutes. A dark precipitate was formed, and the product was washed with water and ethanol three times, dried at room temperature, and calcined in air at 320 or 400 °C for 6 h to produce a nanoporous Au film. The calcination reactions were conducted in a furnace at a heating rate of 1 °C min^{-1}.

2.6. Characterization

The ^1H NMR spectra were recorded at room temperature on a Bruker AM 500 (500 MHz) spectrometer, using the residual proton resonance of the deuterated solvent as the internal standard. The Fourier transform infrared (FTIR) spectra of the polymer films were recorded using the conventional KBr disk method. The film used in this study was sufficiently thin enough to obey the Beer–Lambert law. FTIR spectra were recorded using a Bruker Tensor 27 FTIR spectrophotometer; 32 scans were collected at a spectral resolution of 1 cm^{-1}. The IR spectra of the samples were recorded at elevated temperatures using a cell mounted within the temperature-controlled compartment of the spectrometer. Thermogravimetric analysis (TGA) was performed under nitrogen or air using a TA Q50 operated at a heating rate of 20 °C min^{-1} over the temperature range of room temperature to 800 °C. The rate of nitrogen or air flow was 60 mL min^{-1}. UV–Vis spectra (DU700, Beckmann) were used to characterize the Au NPs aggregate phenomena from 400 to 750 nm. The size distribution of the Au core in the aggregates was measured by transmission electron microscopy (TEM) (JEOL JEM-1200CX, JEOL JEM-200CX). To observe the phase structures of the nanoporous Au films, all specimens were examined with a FEI Quanta 200 environmental scanning electron microscope operated at 20 kV.

3. Results and Discussion

3.1. Synthesis of PS-*b*-PBO Copolymer and Reaction with 4-ATP

Figure 1 shows the ^1H NMR spectra of PS-*b*-PB and PS-*b*-PBO diblock copolymers, wherein the signals due to the aromatic protons were observed at 6.5–7.1 ppm for the PS block. These signals did not change after epoxidation with *meta*-chloroperoxybenzoic acid. However, the double bonds ($HC=CH_2$) from polybutadiene were located at 4.9, 5.1, and 5.3 ppm, and these signals had almost entirely disappeared after the epoxidation with *meta*-chloroperoxybenzoic acid. New signals were observed at 2.5 and 2.7 ppm, corresponding to the epoxide group of PBO segment in the PS-*b*-PBO copolymer. Figure 1 also provides assignments of all of the other signals for the hydrogen atoms of PS-*b*-PB and PS-*b*-PBO block copolymers. FTIR analysis in Figure 2 confirmed the epoxidation of block copolymer, with the characteristic signals for the C=C bond and the epoxide group. The characteristic absorption bands of the allyl group of the PB segment that appear at 3186 (stretching of =C–H bonds), 1636, and 1658 cm^{-1} (stretching of C=C bonds) had disappeared after epoxidation; in addition, a new band for the epoxide ring of the PBO segment appeared at 914 cm^{-1}. After reaction with 4-ATP, the epoxide peak intensity at 914 cm^{-1} of PBO had decreased, and the broad band absorption at ≈3364 and ≈3464 cm^{-1} was observed, assigned to the secondary amine and hydroxyl from the ring opening reaction of the epoxy group and amine group from the 4-ATP, indicating that the reaction occurred under thermal conditions without the need for a catalyst. The curing reaction was also summarized in Scheme 1.

3.2. Micelle Morphologies of PS-*b*-PBO and PS-*b*-PBO–ATP in THF–CH_3CN Mixture

Because of the different nature of the PS and PBO blocks, this copolymer is expected to undergo self-assembly into nanosized micelles in the presence of a selective solvent. As a general procedure, the block copolymer in this study was first dissolved in a good solvent for both blocks, at a typical concentration of 1 mg mL^{-1}. A second nonsolvent, a poor solvent for one of the blocks, was then added to the polymer solution very slowly. In the THF–CH_3CN (1:2) solvent system, PS-*b*-PBO was first dissolved in the

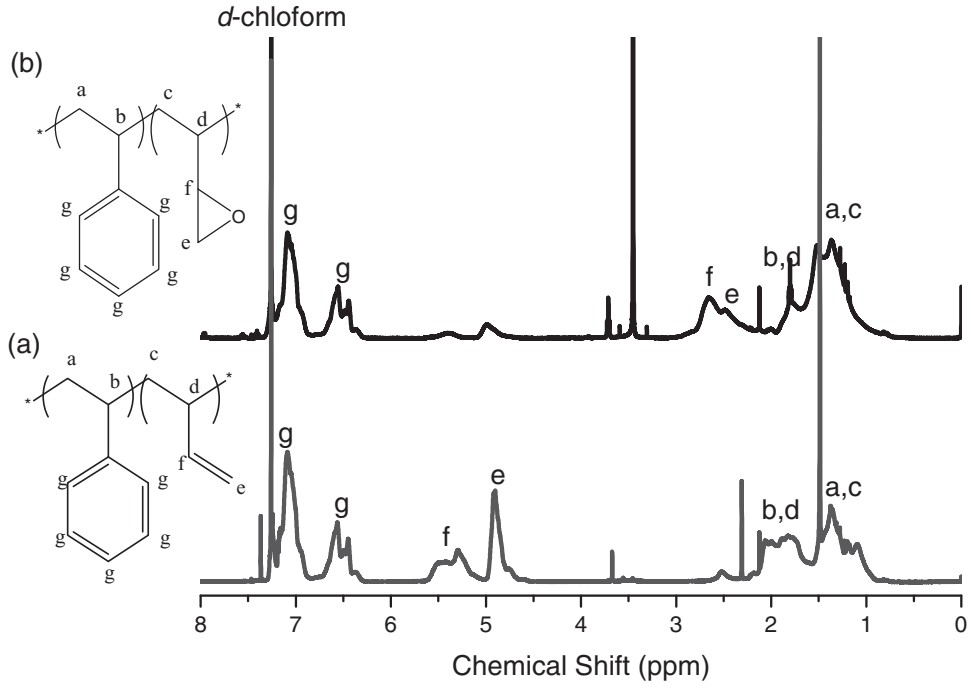

Figure 1. ^{1}H NMR spectra of (a) PS-*b*-PB and (b) PS-*b*-PBO.

common solvent of THF, and then the nonsolvent CH_3CN was added slowly to induce phase separation and aggregation of the PS block. Eventually, the PS block condensed gradually, and the PBO block constituted the outer shell of the micelles. The TEM micrograph of PS-*b*-PBO micelles is shown in Figure 3. Spherical micelles were formed by the diblock copolymer, as would be expected when the shell block length of PBO is longer than core block length of PS. These spheres are nearly identical in size of ≈20 nm.

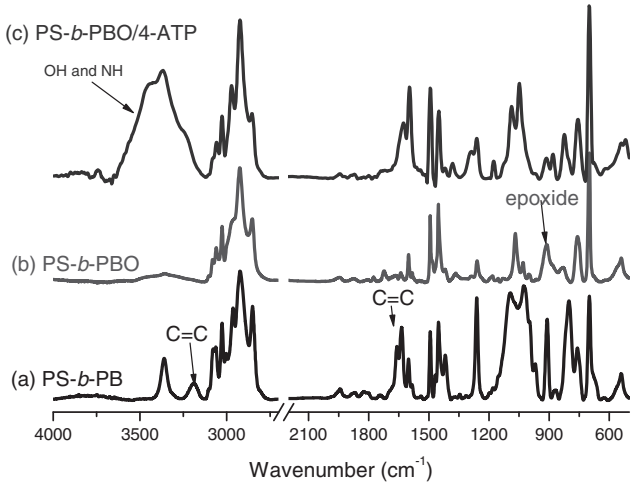

Figure 2. FTIR spectra of (a) PS-*b*-PB, (b) PS-*b*-PBO, and (c) PS-*b*-PBO and ATP.

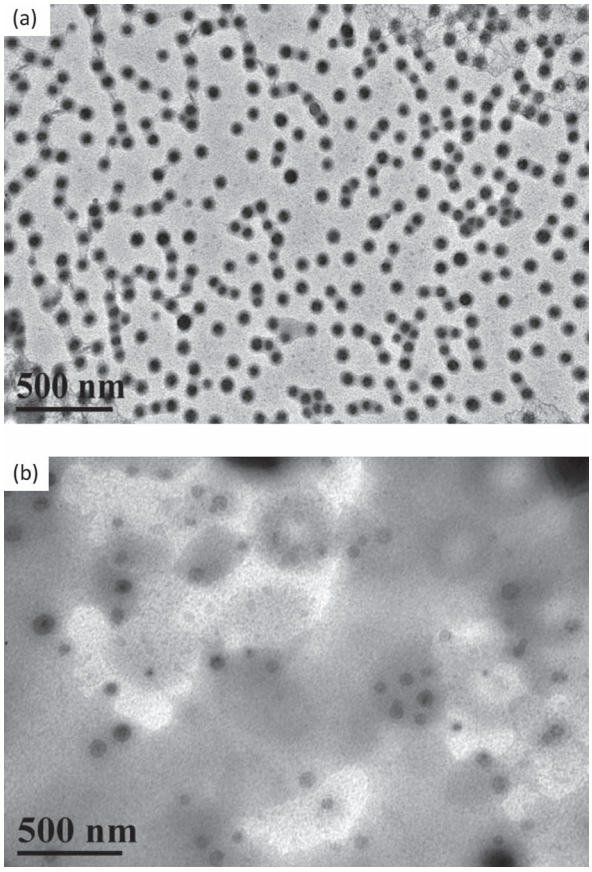

Figure 3. TEM images of (a) PS-*b*-PBO and (b) PS-*b*-PBO and 4-ATP micelles in THF–CH_3CN solutions.

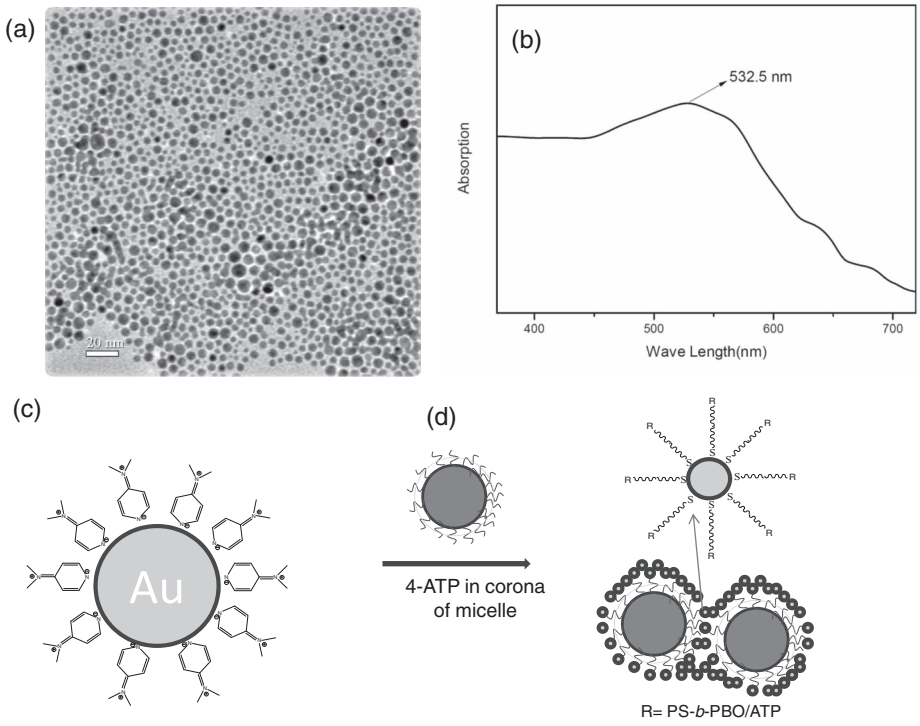

Figure 4. (a) TEM image, (b) UV–Vis spectrum, and (c) the chemical structure of DMAP Au NPs; (d) exchange reaction of PS-*b*-PBO–ATP with DMAP Au NPs.

After reacting with 4-ATP, the morphology of the spheres did not change, but the contrast become more poor because the aromatic ring of 4-ATP is also stained with RuO_4, which has a similar structure to the PS block segment. All results based on FTIR and TEM analyses indicate that the reaction between PBO and 4-ATP had occurred as expected.

3.3. Synthesis of DMAP Au NPs

The DMAP Au NPs used in this study were prepared using the method developed by Gandubert and Lennox.[17] The chemical structure of DMAP Au NPs is shown in Figure 4(c). TEM image of DMAP-functionalized Au NPs is shown in Figure 4(a) and demonstrates that the diameter of the Au core is 5.9 ± 1.2 nm. All DMAP Au NPs were shown to exhibit a size in this range and adopt a closed packed configuration with a significant extent of hexagonal packing that leads to the narrow size distribution. Figure 4(b) shows the UV–Vis spectra of DMAP Au NPs in toluene (300–800 nm). The maximum absorption in toluene is at 532 nm for Au NPs. In the framework of the Mie theory,[18–21] the position of the maximum of the absorption band is determined by the refractive index of the medium surrounding the NPs, while the width is controlled by the particle size. Figure 4(d) shows the synthetic scheme for displacing DMAP with PS-*b*-PBO–ATP micelles at the surface of Au NPs because the thiol–Au bond is stronger than the pyridine–Au bond. This transfer induces the aggregation and precipitation of Au particles.

Figure 5 provides the TGA analyses of PS-*b*-PBO–ATP-modified DMAP Au NPs at different Au NPs content under nitrogen. Clearly, the char yields and thermal stability increased upon increasing the Au NPs content, implying that the Au NPs were effectively transferred

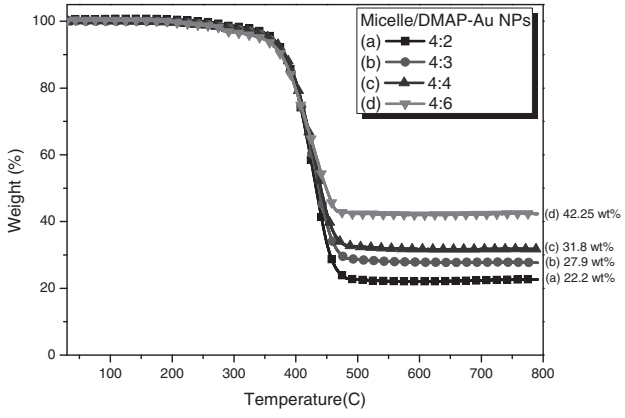

Figure 5. TGA analyses of PS-*b*-PBO–ATP-modified DMAP Au NPs with different amounts of Au NPs under nitrogen.

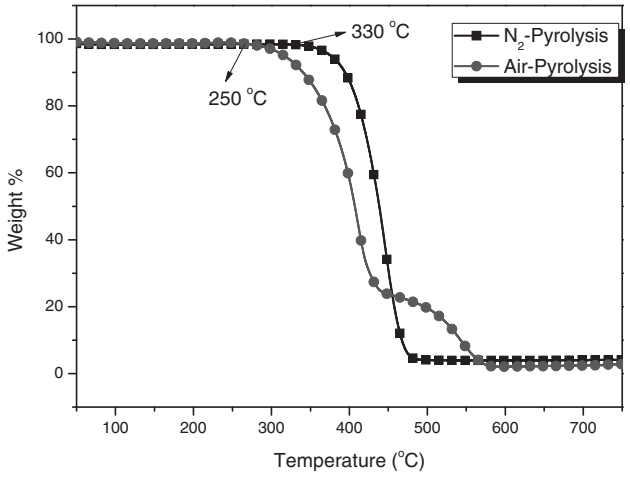

Figure 6. TGA analyses of PS-*b*-PBO–ATP micelle under nitrogen and air.

into the corona of PS-*b*-PBO–ATP micelles. Figure 6 compares the TGA analyses of PS-*b*-PBO–ATP micelle in nitrogen and air. The thermal degradation temperature (5 wt%) of micelle was observed at ≈250 °C in air and ≈330 °C under nitrogen, implying that the template can be easily removed by pyrolysis in both nitrogen and air. In our study, we choose the pyrolysis temperature of 320 °C under nitrogen.

The structure of the nanoporous Au film templated by the PS-*b*-PBO–ATP micelles was also investigated using scanning electron microscopy (SEM). The disordered structure and the nanoporous structure were not observed at a pyrolysis temperature of 400 °C because the Au NPs tend to aggregate to 50 –100 nm diameter clusters, as shown in Figure 7(a). The melting point depression is most evident in NPs, which typically melt at a lower temperature than bulk materials (T_m = 1064 °C for bulk Au).[22] As a result, we can expect that the melting temperature of DMAP Au NPs is lower than 400 °C in this case. From a previous study, we expect that the melting temperature of DMAP Au NPs is ≈370–380 °C based on the particle size.[22] Here, we chose a pyrolysis temperature of 320°C for 6 h under air, and a nanoporous structure was observed, as shown in Figure 7(b). The mean pore size measured from Figure 7(b) was as large as 31.4 ± 2.7 nm.

Figure 8 provides the SEM images of the different ratios of PS-*b*-PBO–ATP DMAP Au NPs prepared at 320 °C for 6 h under nitrogen. Clearly, the nanoporous size decreased with increasing Au NPs content, as expected. SEM images of the surface after pyrolysis revealed the nanoporous structure of the Au film. The obvious contrast between the bright Au film layer and the darker underlying porous structure is shown in Figure 8. This image reveals that the majority of the pores have a diameter between 30 and 100 nm.

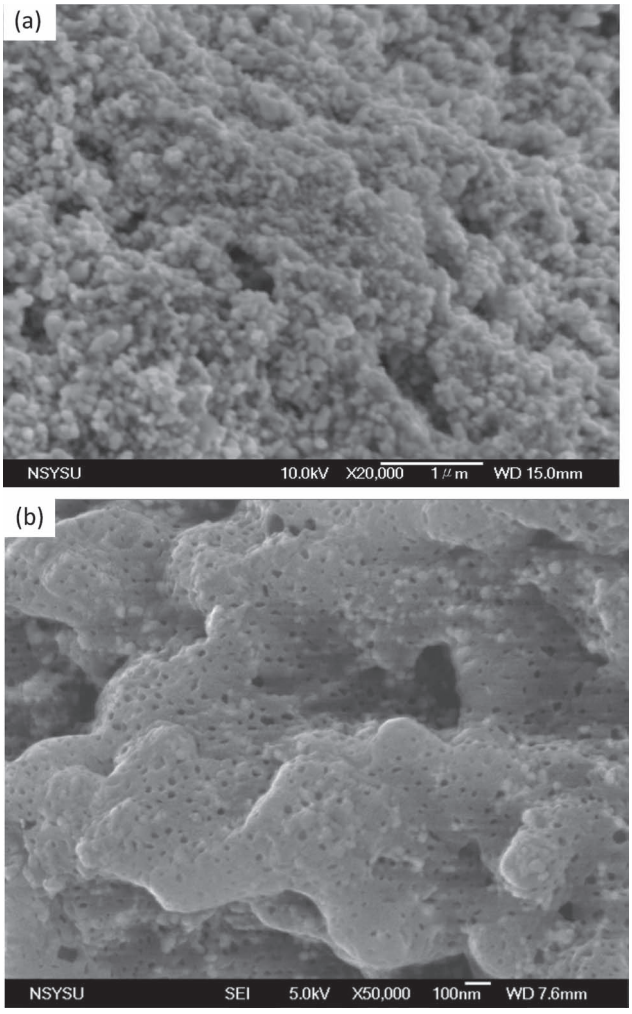

Figure 7. SEM images of PS-*b*-PBO–ATP–DMAP Au NPs (4:3) prepared by pyrolysis at (a) 400 and (b) 320 °C for 6 h under nitrogen.

4. Conclusions

In this study, Au nanoporous films were prepared from Au NPs, whose uniform size distribution could be finely tuned by using DMAP stabilizer molecules. DMAP Au NPs underwent an exchange reaction with 4-ATP PS-*b*-PBO micelles in solutions to form a block copolymer–Au composite. The nanoporous Au film was prepared by the pyrolysis of the diblock copolymer templates. The materials that were fabricated by this method have potential applications as modified electrodes.

Acknowledgements: This study was supported financially by the National Science Council, Taiwan, Republic of China, under contracts NSC 100-2221-E-110-029-MY3 and NSC 100-2628-E-110-001.

Received: August 27, 2011; Revised: November 8, 2011; Published online; December 8, 2011; DOI: 10.1002/macp.201100493

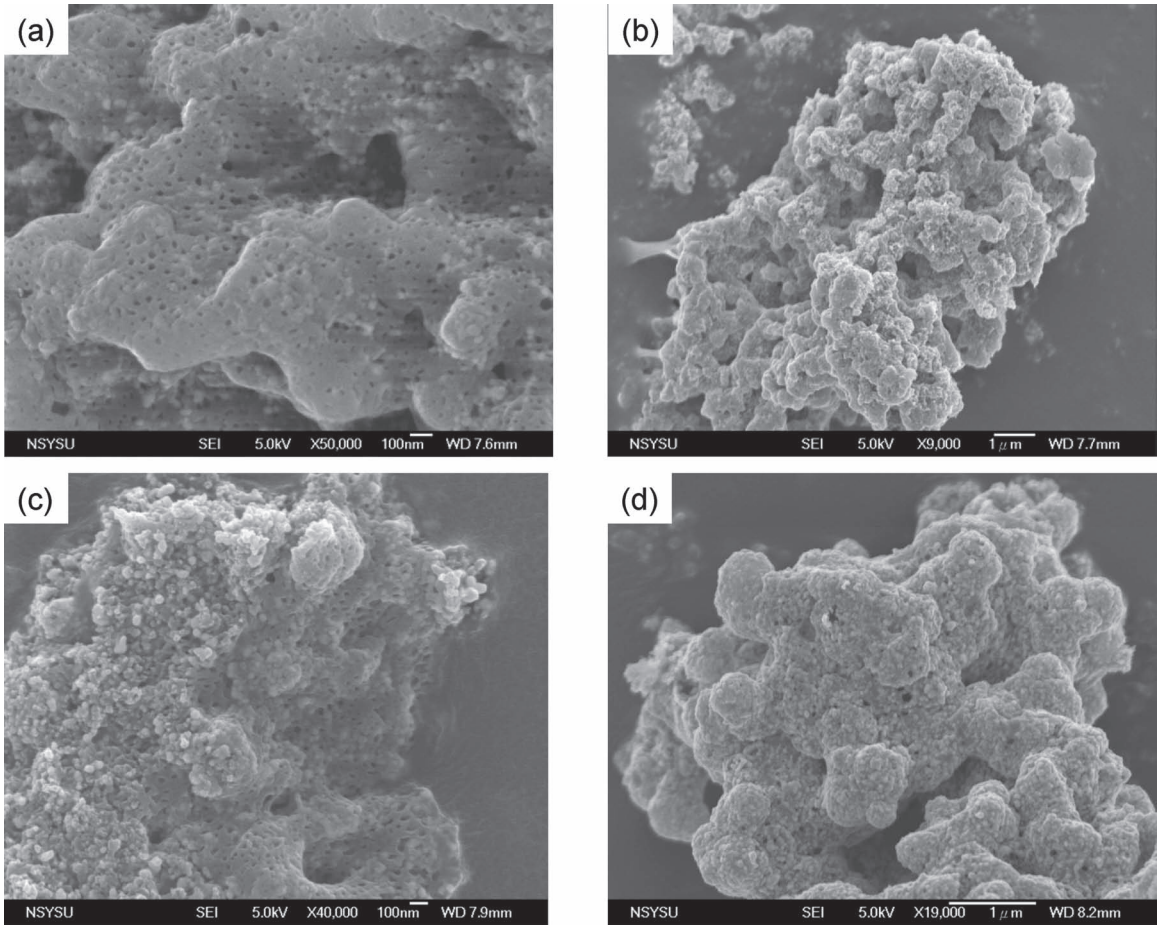

Figure 8. SEM images of PS-*b*-PBO–ATP–DMAP Au NPs = (a) 4:3, (b) 4:4, (c) 4:6, (d) 4:8 prepared using the pyrolysis temperature of 320 °C for 6 h under nitrogen.

Keywords: nanopores; block copolymer; gold nanoparticle; self-assembly

[1] M. Hartmann, *Chem. Mater.* **2005**, *17*, 4577.
[2] H. A. Meng, M. Liong, T. A. Xia, Z. X. Li, Z. X Ji, J. I. Zink, A. E. Nel, *ACS Nano.* **2010**, *4*, 4539.
[3] X. Zhuang, Y. Wan, C. M. Feng, Y. Shen, D. Y. Zhao, *Chem. Mater.* **2009**, *21*, 706.
[4] F. Yu, S. Ahl, A. M. Caminade, J. P. Majoral, W. Knoll, J. Erlebacher, *Anal. Chem.* **2006**, *78*, 7346.
[5] A. Wittstok, J. Bienerb, M. Baumera, *Phys. Chem. Chem. Phys.* **2010**, *12*, 12919.
[6] H. C. Shin, J. Dong, M. L. Liu, *Adv. Mater.* **2003**, *15*, 1610.
[7] A. J. Forty, *Nature* **1979**, *282*, 597.
[8] H. Luo, L. Sun, Y. Lu, Y. S. Yan, *Langmuir* **2004**, *20*, 10218.
[9] H. Zhang, I. Hussain, M. Brust, A. I. Cooper, *Adv. Mater.* **2004**, *16*, 27.
[10] D. Walsh, L. Arcelli, T. Ikoma, J. T. Mann, *Nat. Mater.* **2003**, *2*, 386.
[11] J. T. Zhang, P. P. Liu, H. Y. Ma, Y. Ding, *J. Phys. Chem. C* **2007**, *111*, 10382.
[12] W. Van Zoelen, G. ten Brinke, *Soft Matter* **2009**, *5*, 1568.
[13] W. J. Shin, F. Basarir, T. H. Yoon, J. S. Lee, *Langmuir* **2009**, *25*, 3344.
[14] H. Arora, Z. Li, H. Sai, M. Kamperman, S. C. Warren, U. Wiesner, *Macromol. Rapid Commun.* **2010**, *31*, 1960.
[15] S. C. Warren, L. C. Messina, L. S. Slaughter, M. Kamperman, Q. Zhou, S. M. Gruner, F. J. Disalvo, U. Wiesner, *Science* **2008**, *320*, 1748.
[16] S. W. Kuo, H. Y. Yang, *Macromol. Chem. Phys.* **2011**, *212*, 2249.
[17] V. J. Gandubert, R. B. Lennox, *Langmuir* **2005**, *21*, 6532.
[18] T. Yonezawa, K. Yasui, N. Kimizuka, *Langmuir* **2001**, *17*, 271.
[19] C. H. Lu, S. W. Kuo, C. F. Huang, F. C. Chang, *J. Phys. Chem. C* **2009**, *113*, 3517.
[20] S. W. Kuo, Y. C. Wu, C. H. Lu, F. C. Chang, *J. Polym. Sci., Polym. Phys.* **2009**, *47*, 811.
[21] C. H. Lu, C. F. Huang, S. W. Kuo, F. C. Chang, *Macromolecules* **2009**, *42*, 1067.
[22] K. Dick, T. Dhanasekaran, Z. Zhang, D. Meisel, *J. Am. Chem. Soc.* **2002**, *124*, 2312.